U.S. DEPARTMENT OF THE INTERIOR

U.S GEOLOGICAL SURVEY

Soil Moisture Tendencies into the Next Century for the Conterminous United States

by

Konstantine P. Georgakakos[1,2] and Diane E. Smith[1]

Open-File Report 00-335

 This report is the basis for an article submitted for publication to the *Journal of Geophysical Research - Atmosphere,* that is currently under review.

1 Hydrologic Research Center, 12780 High Bluff Drive, Suite 250, San Diego, CA 92130, USA
2 Scripps Institution of Oceanography, UCSD, CA 92093-0224, USA

August 2000

Soil Moisture Tendencies into the Next Century for the Conterminous United States

Konstantine P. Georgakakos[1,2] and Diane E. Smith[1]

ABSTRACT

A monthly snow-pack and soil-moisture accounting model is formulated for application to each of the climate divisions of the conterminous United States for use in climate impacts-assessment studies. Statistical downscaling and bias-adjustment components complement the model for the assimilation of large-scale global climate model data. Simulations of the formulated model driven by precipitation and temperature for the period 1931-1998 produce streamflows that are broadly consistent with observed data from several drainage basins in the US. Simulated historical soil moisture fields reproduce several features of the available observed soil moisture in the Midwest. The simulations produce large-scale coherent seasonal patterns of soil moisture field-moments over the conterminous US, with high soil moisture means over divisions in the Ohio Valley, the northeastern US and the Pacific Northwest, and with pronounced low means in most of the western US climate divisions. Characteristically low field-standard-deviations are produced for the Ohio Valley and northeastern US, and the Pacific Northwest in winter, and the southwestern US in summer. Differences in extreme standardized anomalies of soil moisture over the historical record range possess high values (2.5 - 3) in the central US where the available water capacity of the soils is high.

An application of the model to exemplify the methodology for determining projected US monthly soil moisture fields under control and greenhouse gas forcing is also documented. Climate simulations of the coupled global climate model from the Canadian Centre for Climate Modeling and Analysis were used for these sensitivity examples. The climatology of the control-run soil moisture fields reproduces several characteristic features of the historical soil moisture climatology. Simulations with forcing by a 1% greenhouse-gas-increase scenario show that for at least the first few decades of the 21st Century somewhat drier-than-present soil conditions are projected, with highest drying trends found in the southeastern US. The soil moisture deficits in most areas are of the same order of magnitude as the soil moisture field-standard-deviations arising from historical natural variability. In a companion paper (*Brumbelow and A. Georgakakos, 2000*), the monthly soil moisture fields for the historical, control and greenhouse-gas-increase runs are used to initialize a site-specific daily crop yield model at the start of the growing season. Assessments of potential impacts of climate variability and trends on irrigation requirements and crop yield across the conterminous US are made.

Keywords: *soil moisture, climate change, crop yield, hydrologic modeling, impacts assessments*

[1]Hydrologic Research Center, 12780 High Bluff Dr., # 250, San Diego, CA 92130
[2]Scripps Institution of Oceanography, UCSD, La Jolla, CA 92093-0224

INTRODUCTION

The questions that motivated the present study are:

(a) *What are the tendencies and sensitivities of conterminous-US soil moisture over the historical period of record, and what are expected tendencies and sensitivities given climate forecasts into the next century?*
(b) *What is the impact of such variability on irrigation requirements and crop yield in the US?*

The present paper develops a framework and models to address the first question on monthly scales and over the climate divisions of the conterminous US. A companion paper (*Brumbelow and A. Georgakakos, 2000*) uses the soil moisture fields produced and appropriate crop yield models to address the second question.

It is long recognized that soil moisture regulates land-surface energy and moisture exchanges with the atmosphere and has a key role in flood and drought genesis and maintenance (*Walsh et al. 1985; Karl, 1986; NRC, 1991; Chen and Avissar, 1994; Georgakakos et al. 1995; Betts et al. 1996; Caporali et al. 1996; Huang et al. 1996; Eastman, J.L., et al. 1998;* and others). Soil moisture deficit plays a significant role in regulating plant transpiration and, consequently, constitutes a diagnostic variable for irrigation design (e.g., *Dagan and Bresler, 1988; Protopapas and A. Georgakakos, 1990*). High extremes of soil moisture are associated with high potential for flooding and hazardous conditions (e.g., *Georgakakos and Bae, 1994*).

Although the importance of soil moisture for hydrologic science and applications cannot be overemphasized, there are few long-term and large-scale measurement programs for soil moisture that provide in-situ profile data suitable for hydroclimatic analysis and design in the US (e.g., *Holinger and Isard, 1994; Georgakakos and Baumer, 1996*) and abroad (*e.g., Vinnikov and Yeserkepova, 1991*). Active and passive microwave data from polar orbiting satellites or reconnaissance airplanes do provide estimates of surface soil moisture with continuous spatial coverage. They are limited in that they only measure soil moisture within the first few centimeters from the soil surface, and are reliable when vegetation cover is sparse or absent (e.g., *Owe et al. 1988; Ulaby et al. 1996; Jackson and Le Vine, 1996; Owe et al. 2000*). As a consequence of the lack of suitable observations, most of the continental-scale studies in hydroclimatology, including the present study, use estimates of soil moisture produced by a variety of models ranging from the land-surface components of global climate models (e.g., *Roads et al. 1994; Shao and Henderson-Sellers, 1996; Dirmeyer et al. 1999)* to conceptual hydrologic models (e.g., *Kunkel, 1990; Milly, 1994; Schaake et al. 1996; Huang et al. 1996; Yates, 1997*). Of these models the model formulated in *Huang et al. 1996* is one that comes close to addressing the objectives of the present study. Apparently it is the only one appropriate for climate division scales that is being used and validated in an operational environment by the Climate Prediction Center of NOAA (http://www.cpc.ncep.noaa.gov/soilmst/cas_text.html and http://www.cpc.ncep.noaa.gov/soilmst/cas_verif.html). Our present modeling work generalizes further that formulation.

Previous modeling and observational studies have shown the rich behavior of soil moisture variability over a range of scales (e.g., *Hills and Reynolds, 1969; Rodriguez-Iturbe et al. 1991; Vinnikov and Yeserkepova, 1991; Georgakakos et al. 1995; Cayan and Georgakakos,*

1995; Rodriguez-Iturbe et al. 1995; Guetter and Georgakakos, 1996; Huang et al. 1996; Vinnikov et al. 1996). In the present study we revisit this problem on continental scales with new physically-based formulations suitable for use with climate-division and global climate model data, and accounting for snow accumulation and ablation in winter and spring. The macroscale hydrologic model is formulated in the next section and it is suitable for application to continental regions with spatial resolution of a few thousand square kilometers and temporal resolution of a month. The model includes soil moisture, runoff and snow accumulation and ablation components. It is forced by precipitation, temperature and potential evapotranspiration. It utilizes spatial digital data of soil texture and plant cover, and when applied over the conterminous US for the historical period it is forced by climate division data. No site-specific calibration is applied to the model results and an estimate of model effectiveness is obtained by comparing simulated and observed runoff production in various catchments in the US and simulated and observed soil moisture for Illinois. Global climate model (GCM) output is used to force the model for future periods, and components are formulated in section 2 for downscaling and uncertainty estimation in the forcing fields. It is noted that the newly formulated macroscale hydrologic model offers the advantage over the land-surface components of global climate models that it allows considerations over scales smaller than the grid size of the GCM (order of 10^5 km^2).

The output from both a control climate model run (simulating present conditions for the future), and a greenhouse gas increase run (1% per year increase in CO_2, accounting for the direct forcing effects of sulfate aerosols) is used as the input to the hydrologic modeling system. Section 3 presents an analysis of the ensuing impacts on simulated soil moisture variability across the US, and section 4 contains concluding remarks. It must be emphasized that it is uncertain whether present day climate models are capable of simulating reliably future climatic changes on regional scales in extratropical regions (e.g., *Takle and Mearns, 1995; Risbey and Stone, 1996; Yu and Mechoso, 1999*). Furthermore, attributing the observed climate change to specific natural or anthropogenic forcings (greenhouse gas emissions and land-use/land-change) is impossible at present as it requires coupled global climate models with improved physics and the availability of large simulation ensembles (e.g., *van Dam, 1999*; *Barnett et al. 2000*). As such, the part of the present study concerning future assessments (as all such assessment studies) should be considered a sensitivity analysis of soil moisture variability under a variety of simulated future scenarios of surface precipitation and temperature. Nevertheless, because of the formulation of a component for bias adjustment of climate model surface precipitation and temperature from past observations (section 2), the present methodology will be valid for future periods when the statistical parameters of these relationships do not change substantially in the next few decades.

New elements of the present study are:

(a) Parsimonious macroscale snow pack and soil moisture models using soils and plant cover spatial databases and with components for statistical downscaling and bias-adjustment of climate model data.

(b) An integrated methodology for assessing site-specific irrigation requirements and crop yields in the US under a variety of climate scenarios (*see also companion paper by Brumbelow and A. Georgakakos, 2000*).

FORMULATION

The modeling philosophy consists of the following elements:

(a) For soil water estimation, one-dimensional considerations along the vertical are adequate.

(b) Large-scale variability of relevant soil and land-cover properties are quantified and incorporated into the modeling procedure.

(c) The model is verifiable at its scale of applicability with observed data of flow and/or soil water.

(d) The model forcing consists of variables with historical data that conform to the requirements of the assessment goals set for soil water variability (e.g., monthly data, typical of GCM output fields).

(e) To the extent possible the GCM forcing is adjusted for spatial-scale effects and for model uncertainty before it is used to force the hydrologic model.

The approach followed in this work follows along the lines of operational soil moisture modeling that was used in *Huang et al. 1996*, which does not include soil surface energy balance modeling but uses the concept of potential evaporation instead. This was done for mainly two reasons: (a) historical data for climate divisions are typically temperature and precipitation; (b) energy balance components for soil moisture modeling require radiation input from historical data and from GCMs and in both cases this input is much more uncertain than temperature (interpolation from sparse observations to climate division scales is a problem for the historical data, and cloud radiation processes are the problem in GCMs as *Barnett et al. 2000* state). We generalize the approach of *Huang et al. 1996* in several respects: (a) we have added a snow accumulation and ablation component; (b) we did away with model components requiring calibration with local data and instead used process-model formulations relying on available spatial digital terrain and land-use land-cover data.

Soil Moisture Model

For the purposes of this work, the basic accounting unit is a climate division of the United States (Figure 1). The soil moisture model assigns a characteristic soil moisture content in each division on the basis of its dominant soil and plant cover characteristics. The state of the model is the soil moisture content q (m^3/m^3)characterizing the soil column within a division during a certain month. The forcing variables are the precipitation plus snowmelt rate, r (mm/mo), and the atmosphere's potential rate for evaporation, e_0 (mm/mo). The latter is modified to reflect plant ground cover. Water availability in the soil column then determines the actual evapotranspiration rate e from the soil.

Surface runoff, q (mm/mo), is generated as a result of soil water availability and difference in average rates between infiltration and precipitation over a month. Baseflow, b (mm/mo), and deep groundwater leakage, g (mm/mo), are produced throughout the soil column to accommodate infiltration rates and large-scale catchment geometry and stream topology.

The equation for the conservation of soil water volume in a soil column characterizing a model division is:

$$Z_T \frac{d(q(t)-q_w)}{dt} = r(t) - e(t) - q(t) - b(t) - g(t) \quad (1)$$

where Z_T (m) is the modeled soil depth, and $q(t)$ is the soil moisture content of the soil at time t. The wilting-point soil-moisture content q_w is defined as the moisture that the soil retains at a –1.5 MPa matric potential. Moisture contents less or equal to this moisture content are not available for evapotranspiration. Together with the saturation soil moisture content, q_s, and the field capacity moisture content, q_f, the wilting point defines the range of soil moisture, which is available for use by plants and for the generation of gravity flow in the soil.

The total surface and subsurface runoff, U_c, is given by:

$$U_c(t) = q(t) + b(t) \quad (2)$$

It is presumed that within the monthly time scale of model application, the climate-division flows are efficiently transported to the sea or evaporate en route, and there are no downstream re-entry points into the soil water system.

Equation (1) is a statement of the natural conservation of water, and to obtain estimates of $q(t)$, expressions for the various flow rates through and over the soils are needed. In developing such expressions (or parameterizations) one should consider the available databases, both spatial digital databases and hydrometeorological databases. The parameterizations used presume availability of the following databases: soils and land-use/land-cover digital databases over the conterminous U.S.; monthly climate division data of precipitation and temperature; limited monthly natural streamflow data. The generation of surface runoff is modeled as a highly nonlinear function of soil moisture content:

$$q(t) = \begin{cases} 0 & ; \quad q(t) - q_w < q_s - q_w \\ r(t) & ; \quad q(t) - q_w \geq q_s - q_w \end{cases} \quad (3)$$

For the purposes of this model and in view of its intended application throughout the conterminous U.S., a spatially dominant soil type is identified for each climate division and it is used as representative of the soils in that climate division. Therefore, the values of the moisture parameters of Equation (3) are those corresponding to the dominant surface soil.

To define the baseflow rate, $b(t)$, the approach of *Mohseni and Stefan (1998)* was followed. The idea is to obtain an approximate expression of the baseflow rate in the stream network by using the soil water seepage velocity to define the area adjacent to the streams that contributes to stream baseflow. Steady state balance between source and demand for water forms the underlying principle. The resultant relationship gives baseflow as a function of the average catchment slope, a measure of drainage density and of hydraulic conductivity. The hydraulic conductivity K is a function of the soil moisture content. For this work we used the empirical formulation of *Mohseni and Stefan (1998)* based on *Brooks and Corey (1964) and Brutsaert (1967)*. The unsaturated hydraulic conductivity K is given as a function of the saturated hydraulic conductivity, K_s, and of the relative available moisture content in the soil:

$$K = K_s \left(\frac{q(t) - q_f}{q_s - q_f} \right)^{2a+3} \qquad ; q_f \le q(t) \le q_s \tag{4}$$

where a is a soil dependent parameter, and $K=0$ for $q(t)<q_f$.

Groundwater leakage, g(t), may be defined as a fraction of baseflow according to:

$$g(t) = mb(t) \tag{5}$$

where m is a non-negative model parameter.

The model parameterizations pertaining to the evapotranspiration rate are discussed next. The actual evapotranspiration rate e is a function of the potential evapotranspiration rate e_p, corresponding to a particular plant cover under unlimited water supply. Several methods are available for the computation of potential evapotranspiration with varying data requirements. Constrained by the monthly resolution scale of the data and the availability of meteorological data from long historical databases, we used Thornthwaite's empirical formula to compute a reference potential evapotranspiration (e.g., *Bras, 1990, 224-225*). Earlier continental hydrologic modeling studies (e.g., *Milly, 1994; Huang et al. 1996*) have used this formula with reasonably good results. In addition, temperature is a key output of global climate models and its simulations have reasonably good correspondence with observed data over large scales (*Barnett et al. 2000*).

Once the reference potential evaporation e_0 has been computed, the effects of crop canopy distribution and crop phenology are incorporated in a simple way. The development follows that of *Saxton et al. (1974)*. A monthly coefficient f_{s_i} (i=1,2,…12) is used to specify the fraction of bare soil versus plant canopy for each month for the area of interest. The values of f_{s_i} are plant-type dependent, and Table 1 shows the values used for grasses and agricultural crops (e.g., corn/wheat), and evergreen and deciduous trees. The ability of grasses and corn/wheat to transpire also depends on their degree of maturation and other phenology influences under unlimited water supply. So for the portion of the area that is covered by the canopy in the case of grasses and corn/wheat another parameter, f_{p_i}, is used to account for the aforementioned phenology influences by month. The values of this parameter used in each case and for each month are also shown in Table 1. The values assigned to the coefficients of the moisture stress relationships are based on *Saxton et al (1974)*. Digital land-use/land-cover data may be used in conjunction with digital climate division data to estimate the plant cover corresponding to the dominant soil cover for each division in terms of broad categories for the estimation of the coefficients f_{s_i} and f_{p_i} from Table 1.

In this study, digital soils and land-use/land-cover spatial databases were used for model application over the conterminous U.S. Specifically, the STATSGO (State Soil Geographic) database (*NRCS, 1994, and Miller and White, 1998*) and a digital land-use and land-cover database (*Baily, 1995*) were used to determine the soil class (based on soil texture), depth to bedrock, and type of dominant vegetation class for each climate division. Figure 2 shows the generated parametric digital spatial databases used with the model. Each climate division is characterized by a single value for all the parameters shown. No attempt was made to account for the spatial variability of these parameters within climate divisions.

The large spatial inhomogeneity in soil properties for field scales (greater than a few m^2) has been well documented (e.g., *Cosby, et al. 1984; NRC, 1991*). Even for a particular soil class (e.g., loam), a range of values for soil moisture parameters (q_s, q_f, and q_w) and a wider range of values for saturated hydraulic conductivity K_s have been measured. Catchment scale values are not directly observable for use by the model, the model is a simplification of complex natural processes, and there is a long data interval of one month used. Thus, for site specific studies, the model-appropriate estimates of parameters should be obtained on the basis of historical flow and soil moisture data for each climate division, through a process known as model calibration.

However, soil moisture databases with at least ten years of data are not available in the conterminous United States except for the prototype one developed for the State of Illinois (*Holinger and Isard, 1994*). The emphasis in this work is the behavior of soil water under assumed future forcing generated by climate models and which carries substantial uncertainty. Also, climate divisions do not necessarily correspond to hydrologic basins with measured outflow data. For these reasons, the approach taken was to use nominal parameter values for all the runs made (see Table 2). Thus, no parameter estimation was conducted and our most reliable results pertain to the relative changes of model output behavior when forced by various input scenarios. To establish a range for expected model errors when using nominal parameters, we do compare the model generated monthly runoff over the historical period with observed monthly runoff from selected catchments embedded within or embedding climate divisions of similar area. We also show an intercomparison of the model simulations with the Illinois soil moisture data. These results are presented in section 2.3 after we formulate the snow-pack model component.

Snow Model

Within the conterminous United States snow processes are important during the winter and spring months in the northern States and in the major mountainous areas (e.g., Appalachian Mountains, Rocky Mountains, and Sierra Nevada Mountains). There is a variety of snow accumulation and ablation models, each with different data requirements (e.g., *Gray and Prowse, 1993*). Thus, models utilizing the full energy balance equations require extensive and intensive data on a variety of meteorological variables such as net radiation, humidity, wind speed, etc. There are empirical index models which utilize individual meteorological variables (such as air temperature) to compute snow melt, which are more suitable for applications with routinely available data. In this work we use an adaptation of the air-temperature-driven model by *Anderson (1973)*. The model uses air temperature to compute components of the snow cover energy and mass balance. It is noted that air temperature is used as an index to energy exchange across the snow-air interface and not only to snow cover outflow. The original model was designed for use with six-hourly data. It included rain-on-snow melt events and snowmelt during interstorm periods. For the present study, monthly data of precipitation and temperature are available and, for this reason, several modifications were made to the original model as described next.

The snow accumulation and ablation model is a discrete time model operating on a monthly basis. It accounts for the following quantities at the beginning of month t: S_t, snow cover water equivalent; D_t, snow pack heat deficit expressed in mme or mm of energy per unit area (1 mme is the energy required to melt or freeze 1 mm of ice or water at 0 ^{o}C or approximately 8 cal cm^{-2}); and A_t, an antecedent temperature index of the temperature within

snow (≤ 0 ^{o}C). The model equations applied to month t, characterized by an average surface air temperature T_t and precipitation P_t, are:

$$S_{t+1} = S_t + P_{x_t} - M_t \tag{6}$$

$$A_{t+1} = A_t + C_4(T_t - A_t)\ ;\ A_t \leq 0 \ \textit{for all } t \tag{7}$$

$$D_{t+1} = D_t + C_{5_i}(T_t - A_t) + \frac{P_{x_t} T_t}{160} + M_t^F\ ; D_t \leq 0 \tag{8}$$

where P_{x_t} is the adjusted snowfall in month t, M_t is the snowmelt during month t, M_t^F is the melt that refreezes in the snow cover, and C_4, C_{5_i} are parameters. The term involving P_{x_t} in Equation (8) is for new snow and exists when $T_t \leq 0$ ^{o}C. Parameter C_4 is in the range $0.1 \leq C_4 \leq 1.0$, with the value of 1.0 reserved for situations when $T_t = A_t$. Regarding the procedure for the solution of the Equations (6) – (8), it is noted that, although melt may be computed for a given month, it may refreeze in whole or in part in that same month if the heat deficit is less than zero.

Ignoring snowmelt due to rain-on-snow events, snowmelt is computed from

$$M_t = M_{f_i}(T_t - T_t^o) \tag{9}$$

where T_t^o is a constant and M_{f_i} is a monthly varying melt factor (in mm ^{o}C^{-1}). The temperature T_t^0 was estimated to be equal to -6 ^{0}C for monthly data intervals based on preliminary analysis using data from catchments in the northern, non-mountainous US.

The snow model formulation used is a substantially simplified version of the *Anderson (1973)* air-temperature index model. Main simplifications, motivated by the length of the monthly time step, are: (a) there is no separate accounting for excess liquid water stored in the snow cover; (b) there are no time delays and attenuation in the outflow of liquid water from the snow cover; and (c) there are no partial snow cover contingencies, as it is assumed that the area either has 100 percent snow cover or it has no snow cover in a given month. The parameters of the model were set to nominal values for all the runs made.

Inference from Model Application to Selected Sites

Streamflow Data

Data from several sites were used to estimate the degree to which the model reproduced monthly flow in natural catchments. The catchments were selected to represent different hydroclimatic regimes and topography across the US and were of size commensurate to that of nearby climate divisions. No site-specific model calibrations were performed and the model parameters were estimated from the spatial databases developed for the nearest climate division. A simple linear reservoir routing model was used to time distribute monthly runoff volumes produced by the model, with the single parameter of the routing model set to the inverse of the basin lag time. Also, for these site-specific studies we adjusted the long-term monthly potential

evapotranspiration rates to close the water balance in each site, as it is known that the Thornthwaite's formulation does generate biases in potential rates (*Milly, 1994; Huang et al. 1996*). Information regarding the test sites is in Table 3 and the results of our simulations as compared to the observations are shown in Figure 3.

In most cases, the potential evaporation adjustment resulted in up to 50 percent higher potential rates in winter and spring, and up to 50 percent lower potential rates in summer. For the case study in Arizona, substantial reduction of potential rates was necessary throughout the year. While the underestimation is expected for the Thornthwaite's formula, sensitivity experiments with daily data for the sites showed that the overestimation in drier regimes is primarily due to the long data interval that does not allow realistic representation of the effects of intermittent convective precipitation regimes in streamflow. The introduction of a parameter for the number of rainy days in a month improves the results, but this parameter depends significantly on climate and it is not available for our sensitivity experiments with GCM output. Such a parameter was not used for this study. Also, for the sensitivity studies with historical climate division data and with GCM data, all the monthly adjustment factors for potential evaporation were set equal to the nominal value of 1 for all the climate divisions.

An additional note is necessary regarding the differences in spatial extent among climate divisions in the eastern and western US. In the latter case, the large areas of climate divisions contribute to the errors of the model in regions and periods with strong convective regimes. Also, our neglecting the variability of soils and plant cover within each division has more pronounced effects for the larger divisions in the West.

The simulated and observed monthly flow cycles in Figure 3 are in broad agreement for all cases and months, and the monthly differences are within the range obtained by other validation studies (e.g., Shao *and Henderson-Sellers, 1996; Dirmeyer et al. 1999*). The cross-correlation coefficient, r, between monthly observed and simulated streamflow suggests that the simulated flows explain at least 45% of the observed flow variance, with the lowest value obtained for the Arizona case study and the highest value obtained for the 3^ox3^o area in Oklahoma.

Soil Moisture Data

Data from the Illinois long-term soil-moisture-observing network were also used to determine the character of model errors in soil moisture. It is noted that this area has non-negligible snow cover in winter. Three measurement sites in and near climate division 71 (which contains Salt Creek in Illinois, see Table 3 and Figure 3) provided soil water data. Depth-averaged soil moisture was used to produce monthly averages at each site. The arithmetic average of the values at the three sites was then computed for each month to produce monthly soil moisture estimates for climate division 71 from observed data. These estimates are compared to those generated by the model for climate division 71 in Figure 4.

The model results are in general agreement with the observed data with excellent time matching of the highs and lows of soil moisture. During the first four years of record, soil moisture monthly cycles are very well reproduced in amplitude and phase. During the period from 1986 through 1998 although the phase of the cycle continues to be reproduced well, there is significant overestimation of the amplitude of the monthly cycle by the model (40-70 percent). The model does reproduce the variations of the cycle lows well throughout the period. It is less successful in doing so for the maxima of the cycle. Similar results were obtained for other divisions in Illinois (see Table 4) with a 25 - 65 % explanation of observed monthly variance.

In spite the noted model shortcomings, the results obtained show non-negligible skill in reproducing both runoff and soil moisture in a variety of conditions. The model's physically-based nature allows for its use in sensitivity studies to examine the effect of various forcing scenarios to soil moisture simulations. In that respect the model is commensurate with the GCM forcing in that it is not calibrated regionally, but that regional differences in its parameters are a result of using the spatial digital soils and pant-cover databases of Figure 2.

Coupled Global Climate Model Forcing

In order to extend the analysis in the future, the monthly simulations provided by a coupled ocean-atmosphere global climate model (CGCM) for the period 1931-2100 were considered to determine the input to the macroscale hydrologic model for future times. The particular CGCM model used was developed at the Canadian Centre for Climate Modeling and Analysis with a resolution of approximately 3.75^0 x 3.75^0. It is documented at the web site: www.cccma.bc.ec.gc.ca/cgi-bin/cgcm1.

It is apparent that for the eastern United States, a grid box of this particular CGCM model contains several climate divisions (see Figure 1). Direct use of the information in the CGCM simulations cannot be made (at least) for monthly precipitation because of *(a)* the disparity of scale between the resolution of the CGCM fields and the required input to the macroscale hydrologic model at climate-division scales, and *(b)* the considerable uncertainty in the CGCM simulations of precipitation and temperature. For example, the coarser CGCM fields would considerably smooth highly localized extreme monthly precipitation rates. Figure 5 shows the cross correlation between the GCM monthly precipitation simulations at the GCM grid-box level and the corresponding monthly observed precipitation computed from the observed climate division data corresponding to each GCM grid-box. Maximum values are approximately equal to 0.4. The CGCM explains less than 16 percent of the monthly variability of the observed precipitation field on the 3.75^0x3.75^0 scale. Better precipitation simulations are shown for the southern Appalachians, Upper Great Plains, and the northern Pacific Coast.

Direct comparison of CGCM simulations and aggregated climate division data for individual grid boxes reveals that there is very little association between the time series at those scales for most of the US. Linear regression relationships of observed vs. CGCM precipitation data were obtained for four grid boxes randomly selected in Illinois, Oklahoma, northern California and Georgia. The results show that the regressions have a positive intercept on the observed precipitation axis (the CGCM simulations are biased high), and the regression correlation coefficient ranged from less than 0.1 for Georgia to about 0.25 for the Midwestern grid boxes to about 0.4 for northern California.

Given these results for the CGCM grid box scales, direct use of the CGCM precipitation monthly simulations as input to the nonlinear macroscale model will result in highly uncertain hydrologic fields due to inherent CGCM simulation errors and because of the disparity of scale between the CGCM grid box size and the size of the climate divisions. The latter is particularly true for the eastern and central US where several climate divisions are contained in a single CGCM grid box. It is, however, desirable to use the CGCM information as it is probably the best source of information for future years without observed data (*Barnett et al., 2000*). The following methodology was used in an effort to reduce the noise in the CGCM information and to represent it reliably in the input to the macroscale hydrologic model. It is used with each climate division. *Chen et al. 1998* shows that such methodologies produce useful results for surface precipitation.

The parameters of linear regressions between aggregate climate division precipitation (or temperature) and CGCM simulations of precipitation (or temperature) for each month of the year have been estimated using the historical data for the period 1931-1998 for all the divisions and GCM nodes within the conterminous US. Thus, if we denote by $P_a(i,t,m)$ the aggregate precipitation (or temperature) corresponding to CGCM node i in year t and month m, and by $P_g(i,t,m)$ the analogous quantity simulated by the CGCM, the regression equations are of the type:

$$P_a(i,t,m) = a_{1,m} P_g(i,t,m) + a_{0,m} + v(i,t,m) \tag{10}$$

where $a_{1,m}$ and $a_{0,m}$ are regression parameters and $v(i,t,m)$ is a random error. The estimation of the regression parameters (they do not depend on particular nodes) is done using the historical climate division data, $P_D(j,t,m)$, of precipitation or temperature, and the concurrent CGCM simulations of these quantities over the entire conterminous US. The climate division data are aggregated to the level of the CGCM grid boxes using:

$$P_a(i,t,m) = \frac{1}{N_i} \sum_{j=1}^{j=N_i} P_D(j,t,m) \tag{11}$$

where N_i is the number of climate subdivisions that are closest to the i^{th} CGCM grid node. This number is large in the eastern US while it may be as low as 1 in the West. There is an association table that links each climate division number j to the corresponding CGCM grid node number i.

For precipitation, the regression correlation coefficient ranges from about 0.23 in August to about 0.42 in June, with most of the months having coefficient values of about 0.35. Even though the values are small they are significant given the abundance of data used in their estimation, and they reflect the difficulties associated with downscaling a highly intermittent field such as precipitation. The intercept estimates ranged from about 0.9 to about 1.5.

The next step involves the computation of climate division residuals for each climate division j associated with CGCM node i as follows:

$$R_D(j,t,m) = P_D(j,t,m) - \hat{P}_a(i,t,m) \tag{12}$$

where $\hat{P}_a(i,t,m)$ represents the regression estimate of the aggregate climate division precipitation (or temperature) for node i computed using the estimated regression parameters. Long term averages, $\hat{R}_D(j,m)$, and standard deviations, $S_D(\hat{j},m)$, of $R_D(j,t,m)$ may be computed for each climate division, for each of precipitation and temperature variables, and for each month of the year:

$$\hat{R}_D(j,m) = \frac{1}{T} \sum_{t=1}^{t=T} R_D(j,t,m) \tag{13}$$

$$\hat{S}_D(j,m) = \frac{1}{T}\sum_{t=1}^{t=T}(R_D(j,t,m) - \hat{R}_D(j,m))^2 \qquad (14)$$

where T is the number of years of record. The standardized remainder vector $\underline{e}_D(j,t,m)$, with elements the precipitation and temperature components, may then be modeled as a vector autoregressive process:

$$\underline{e}_D(t+1) = A \cdot \underline{e}_D(t) + H\underline{x}(t+1) \qquad (15)$$

with

$$e_{D_{1,2}}(j,t,m) = (R_{D_{1,2}}(j,t,m) - \hat{R}_{D_{1,2}}(j,m)) / \hat{S}_{D_{1,2}}(j,m) \qquad (16)$$

where subscripts 1 and 2 denote precipitation and temperature, matrix A and matrix H are parameter matrices, $x(j,t,m)$ is a normal random vector with zero mean and unit covariance matrix. The elements of parameter matrices A and H are estimated from historical data. Equation (15) is applied sequentially for each month of each year of record.

For the determination of climate division input data for future years for division j, the reverse process is followed:

(1) For each of precipitation and temperature, compute $\hat{P}_a(i,t,m)$ from regression (10) using estimated parameters, and the CGCM future simulations for node i corresponding to climate division j.

(2) Estimate the future precipitation (or temperature) for the climate division, $P_D(j,t,m)$, as follows:

$$P_D(j,t,m) = e_{D_{1,2}}(j,t,m)\hat{S}_{D_{1,2}}(j,m) + \hat{R}_{D_{1,2}}(j,m) + \hat{P}_{a_{1,2}}(i,t,m) \qquad (17)$$

The methodology outlined preserves the mean trends in the future GCM simulations, adjusts biases in the GCM predictions due to scale and other effects, and incorporates the variability on smaller scales. It does assume that the historical second moment properties of $R_D(j,t,m)$ are preserved in the future period, and this is the primary condition for its validity when applied to future periods. Thus, our analysis of future projected scenarios will be limited to the first few decades of the 21st Century.

RESULTS AND DISCUSSION

Three runs of the macroscale hydrologic model were made for all the climate divisions of the conterminous United States with valid data and using nominal parameters. There are 344 climate divisions of which 17 do not have valid data during the historical period and were not considered in the analysis (see also *Huang et al. 1996*). The first run was made with data from the historical period 1931-1998 and using forcing from the observed climate division

precipitation and temperature data. A second run was made with forcing from the CGCM1 control run using present day greenhouse gas emissions. The last run of the macroscale hydrologic model used forcing from the CGCM1 greenhouse-gas-increase run, which assumed 1 percent increase in CO_2 per year including the direct effects of sulfate aerosols. For the last two runs the downscaling and bias adjustment component of the macroscale model (see section 2.4) was active. In the following we present relevant results from these three runs. More detailed analyses of the historical dataset are in progress and will be reported elsewhere.

Historical Run

To describe the spatial variability of soil moisture we compute the mean and standard deviation of the climate-division soil moisture for the model-run period and display it over the conterminous US climate divisions through a geographic information system. Also obtained are maps of the difference between the highest and lowest deciles of soil moisture anomalies (value minus the corresponding long-term monthly mean) over the run period. The latter measure is appropriate for characterizing the range of variability over each climate division.

Figure 6 shows the mean divisional soil moisture for the historical period for January (upper left panel) and June (lower left panel). The unit of soil moisture is m^3/m^3. There is a well-defined trend for moist conditions for most of the eastern US and the Pacific Northwest. As expected, January soil moisture is higher than June soil moisture, with the largest changes occurring along the West Coast and in the Southwest. Soil moisture means span the range from about 0.10 to about 0.45. The corresponding historical soil moisture standard deviations are also shown in Figure 6 for January (upper right panel) and June (lower right panel). Least soil moisture variability is obtained for the eastern US and the Pacific Northwest in January, and for the California and the Southwest in June. The winter estimates of low standard deviation denote consistently moist regional conditions, while the summer low standard deviations correspond to consistently dry regions. Overall the standard deviation is a small fraction of the soil moisture mean except in the driest southwestern regions during summer.

The range of extreme variability in soil moisture may be described by the difference between the upper 10^{th} percentile and the lower 10^{th} percentile of standardized anomalies for each division. The bottom panel in Figure 6 shows the map of such differences over the conterminous US. It may be seen that the central US, portions of the Southwest and Florida exhibit the largest differences. This is likely the result of extreme forcing and of large available water capacity in the soils.

Future Scenario Runs

The soil moisture means for the control run and for the period 1999-2060 are shown in Figure 7. The results resemble substantially those in Figure 6 corresponding to the historical climate division forcing with the summer soil moisture being somewhat higher for the control run than that of the historical divisional-forcing run. The standard deviations corresponding to the control run forcing are shown in right panels of Figure 7. They resemble the historical run results in Figure 6 for winter but they are dissimilar to those for summer mainly in the dry southwestern US. Differences in extreme deciles in Figure 7 and may be compared to those in Figure 6. The large ranges found for the central and southeastern coastal US are reproduced by the control scenario results. The western US ranges are larger in the control scenario run than they were found for the historical divisional data in Figure 7. These results show that comparing

soil moisture results pertaining to various scenarios with the control-scenario soil moisture results is a valid approach, as the control scenario results are qulitatively similar to those obtained using the historical record.

The soil moisture results for the GCM scenario with a 1% increase of CO_2 concentrations per year (plus sulfate aerosol effects) are shown in Figure 8 (means in left upper panels, standard deviations in right upper panels and differences in extreme deciles in bottom panel). Comparison with the corresponding control scenario results discussed above shows that in several regions of the US there is a drying tendency for soil moisture, particularly in the summer and in the eastern US. Also, the variability of soil moisture (as measured by the standard deviation and the difference in extreme deciles) is greater under the greenhouse-gas increase scenario especially in the eastern US in both winter and summer.

To obtain an aggregate measure of the association of the soil moisture under the control and the greenhouse-gas-increase scenarios, we constructed soil moisture averages over the entire conterminous US for each month of the period 1999-2060 and for both cases. Figure 9 shows the association. There is a strong linear relationship between the soil moisture results corresponding to the two forcing scenarios, with the greenhouse-gas-increase scenario resulting in drying of the soils, especially during times with low soil moisture content (values of 0.27-0.32). To further probe the significance of these results for various regions, we studied the behavior of soil-moisture spatial averages for six sectors of the conterminous US. These were defined based on latitude (LAT) and longitude (LON) as follow:

SouthEast (SE) :	$LAT < 35^0$	$90^0 <$ LON
MidWest (MW):	$LAT > 35^0$	$90^0 <$ LON $< 105^0$
SouthCentral (SC):	$LAT < 35^0$	$90^0 <$ LON $< 105^0$
SouthWest (SW):	$LAT < 40^0$	$110^0 <$ LON
NorthWest (NW):	$LAT > 40^0$	$110^0 <$ LON
NorthEast (NE):	$LAT > 35^0$	LON $< 90^0$

The difference of the monthly values of average soil moisture (control forcing – ramp forcing) was computed for each one of these sectors, and a 5-year moving average operation was applied to the noisy results to reveal significant trends over the study period. Figure 10 shows the smoothed traces for each sector and for the period 1999-2060. Larger positive values indicate drying, while values near zero indicate no significant change in soil moisture from control run conditions (resembling historical conditions as shown earlier). The Figure shows that the Southeast and Northeast regions are expected to exhibit the largest degree of drying over the next half of a century. For those regions, the drying trend is an increasing one for the last decades of the study period. Comparing these results to the means and standard deviations of Figures 6 and 7, we find that the drying changes in soil moisture projected for the next few decades are of the same order of magnitude as the standard deviation due the natural variability and they are small fractions of the soil moisture mean.

Figure 10 also shows evidence of low-amplitude decadal cycles associated with the time series of differences. The amplitudes of these cycles are comparable to the total soil moisture changes over the entire time period, and they may be associated with the North Pacific decadal-scale oscillation noted by *Latif and Barnett (1996)* in the results of coupled global climate model simulations and in observations.

CONCLUDING REMARKS

An important question for planning sustainable agricultural production is: *What are expected tendencies and sensitivities of soil moisture over the conterminous US given climate forecasts for the next century?* To address this question, a macroscale hydrologic model has been formulated which is suitable for use over the climate divisions of the US using monthly data. The model includes soil moisture, runoff and snow accumulation and ablation components. It is forced by precipitation, temperature and potential evapotranspiration. It utilizes spatial digital data of soil texture and plant cover to determine hydrological-model parameters such as soil-moisture field capacity, hydraulic conductivity, and plant phenology seasonal coefficients. Comparison of the model simulations with observations of soil water and flow for the historical period and for various areas of the US reveals generally good reproduction of the observations with minimal calibration.

The macroscale hydrologic model and statistical methods for downscaling coupled global climate model (CGCM) precipitation and temperature fields were used with forcing from the Canadian Centre for Climate Modeling and Analysis CGCM1 to assess the impact to US soil moisture of a one-percent annual increase of greenhouse gas concentrations. The experiments were done for both a control run, assuming present-day CO_2 concentrations, and a greenhouse gas increase run, assuming 1% increase of CO_2 concentrations per year from present conditions and allowing for direct effects of sulfate aerosols. Assessments were made by studying the differences between the soil moisture fields produced, in terms of both tendency and variability for various spatial and temporal scales. The results of this work were used to force regional crop-yield models to study the implications of soil moisture variability and future trends for irrigation requirements and agricultural production (*Brumbelow and A. Georgakakos, 2000, companion paper*).

The following were significant findings of the soil moisture assessment study:

(a) On the climate model grid-box scale, the precipitation fields produced by the control run of the coupled CGCM1 climate model have low cross-correlation coefficients with the observed climate division precipitation (maximum of 0.4 in a few regions of the US). Nevertheless, the soil moisture fields obtained by forcing the hydrologic modeling system with climate model output from the control run are reasonably similar to those obtained from the same modeling system forced by the observed historical climate division data.

(b) There are strong gradients of time-averaged climate-division soil moisture across the conterminous US, with wetter conditions in the east and northwest and drier conditions in the west and southwest. The time standard deviation also exhibits strong seasonal gradients, with low values in the east and high values in the southwest in winter and with low values in the southwest and higher values in the east in summer.

(c) The range of extreme soil moisture variability is highest in the central US and in the coastal southeast.

(d) Assuming a one-percent greenhouse gas increase scenario results in a reduction of soil moisture content for most of the regions of the US. Most significant changes were computed for the eastern US (both southeast and northeast) where drying is shown to have an increasing trend during the period 2025-2060. Even so, the reduction in soil moisture values is expected to be less than 10 percent of the present level of soil moisture, and it is of the same magnitude as the standard deviation of the natural soil moisture variability. It was also

found that the greenhouse gas increase scenario results in regional increases in soil moisture variability, with a regional enhancement of the range of extreme soil moisture values for the eastern US.

Future research is focusing on a more detailed analysis of the variability of the simulated soil moisture fields and their association with El Niño Southern Oscillation indces and surface meteorological variables. Analysis of simulated surface runoff and snow cover is also in progress. An important next step in terms of the soil moisture assessments under projected climate scenarios is to force the macroscale hydrologic model with an ensemble of climate model simulations to allow for an objective estimation of input uncertainty and its effects on projected soil moisture variability. Use of more than one climate model would allow an assessment of the dependence of the methodology proposed to particular GCMs.

Acknowledgements: The research was sponsored by the US Geological Survey through a subcontract by the Georgia Institute of Technology. Additional support was provided by the NOAA-funded Experimental Climate Prediction Center of the Scripps Institution of Oceanography. The authors wish to thank Aris Georgakakos of GIT for his support and useful discussions during the tenure of this research project, and Nick Graham of HRC and UCSD for useful discussions on GCMs. The assistance of Theresa Carpenter of HRC with various computer tasks is gratefully acknowledged. The ideas and opinions expressed herein are those of the authors and do not necessarily reflect those of the US Geological Survey and NOAA.

REFERENCES

Anderson, E.A., 1973: National Weather Service River Forecast System – Snow accumulation and ablation model. NOAA Technical Memorandum NWS HYDRO-17, Office of Hydrology, National Weather Service, NOAA, Silver Spring, MD.

Bailey, R.G., 1995: Description of the ecoregions of the United States. U.S. Department of Agriculture, Forest Service, Miscellaneous Publication 1391, Second ed., revised and enlarged. 108 p. [Available on-line at http://www.essc.psu.edu/soil_info/soil_eco/]

Barnett, T.P., and co-authors, 2000: Detection and attribution of recent climate change, A status report. *Bulletin of the American Meteorological Society,* **80**(12), 2631-2659.

Betts, A.K., Ball, J.H., Beljaars, A.C.M., Miller, M.J., and P.A. Viterbo, 1996: The land-atmosphere interaction, A review on observational and global modeling perspectives. *J. Geophysical Research - Atmospheres,* **101**(D3), 7209-7225.

Bras, R.L., 1990: *Hydrology, An Introduction to Hydrologic Science.* Addison-Wesley Publishing Company, New York, 643 pp.

Brumbelow, K., and A.P. Georgakakos, 2000: An assessment of irrigation needs and crop yield for the United States under potential climate changes. *J. Geophysical Research - Atmospheres, (companion paper).*

Brooks, R.H., and A.T. Corey, 1964: Hydraulic properties of porous media. *Hydrologic Paper 3,* Colorado State University, Fort Collins, Colorado.

Brutsaert, W., 1967: Some methods of calculating unsaturated permeability. *Transactions ASAE,* **10**, 400-404.

Caporali, E., Entekhabi, D., and F. Castelli, 1996: Rainstorm statistics conditional on soil moisture index, Temporal and spatial characteristics. *Meccanica,* **31**, 103-116.

Chen, F. and R. Avissar, 1994: Impact of land-surface moisture variability on local shallow convective cumulus and precipitation in large-scale models. *J. Applied Meteorology*, 33, 1382-1401.

Chen, M., Zeng, X., and R.E. Dickinson, 1998: Adjustment of GCM precipitation intensity over the United States. *J. Applied Meteorology*, **37**(9), 876-887.

Cosby, B.J., Hornberger, G.M., Clapp, R.B., and T.R. Ginn, 1984: A Statistical Exploration of the Relationships of Soil Moisture Characteristics to the Physical Properties of Soils. Water Resources Research, 20(6), 682-690.

Dagan, G., and E. Bresler, 1988: Variability of an irrigated crop and its causes, 3, Numerical simulation and field results. *Water Resources Research*, **24**(3), 395-401.

Dirmeyer, P.A., Dolman, A.J., and N. Sato, 1999: The pilot phase of the global soil wetness project. *Bulletin of the American Meteorological Society*, **80**(5), 851-878.

Eastman, J.L., Pielke, R.A., and D.J. McDonald, 1998: Calibration of soil moisture for large-eddy simulations over the FIFE area. *J. Atmospheric Sciences*, **55**, 1-10.

Georgakakos, K.P., and D.H. Bae, 1994: Climatic variability of soil water in the American Midwest, Part 2, Spatio-temporal analysis. *J. Hydrology*, **162**, 379-390.

Georgakakos, K.P., Bae, D.H., and D.R. Cayan, 1995: Hydroclimatology of continental watersheds, 1, Temporal analyses. *Water Resources Research*, 31(3), 655-675.

Georgakakos, K.P., and O.W. Baumer, 1996: Measurement and utilization of on-site soil moisture data. J. of Hydrology, 184, 131-152.

Gray, D.M., and T.D. Prowse, 1993: Snow and Floating Ice. In Handbook of Hydrology, D.R. Maidment (ed.), McGraw-Hill, Inc., New York, 7.1-7.58.

Guetter, A.K., and K.P. Georgakakos, 1996: Large-scale properties of simulated soil water variability. *J. Geophysical Research - Atmospheres*, **101**(D3), 7175-7183.

Hills, R.C., and S.G. Reynolds, 1969: Illustrations of soil moisture variability in selected areas and plots of different sizes. *J. Hydrology*, **8**, 27-47.

Huang, J., Van den Dool, H.M., and K.P. Georgakakos, 1996: Analysis of model-calculated soil moisture over the United States (1931-1993) and applications to long-range temperature forecasts. *J. of Climate*, **9**(6), 1350-1362.

Jackson, T.J., and D.E. Le Vine, 1996: Mapping surface soil moisture using an aircraft-based passive microwave instrument, Algorithm and example. *J. Hydrology*, **184**, 85-99.

Karl, T.R., 1986: The relationship of soil moisture paameterizations to subsequent seasonal and monthly mean temperature in the United States. *Monthly Weather Review*, **114**, 675-686.

Kunkel, K.E., 1990: Operational soil moisture estimation for the Midwestern United States. *J. Applied Meteorology*, **29**, 1158-1166.

Latif, M., and T.P. Barnett, 1996: Decadal climate variability over the North Pacific and North America, Dynamics and Predictability. *J. Climate*, **9**(10), 2407-2423.

Miller, D.A. and R.A. White, 1998: A Conterminous United States Multi-Layer Soil Characteristics Data Set for Regional Climate and Hydrology Modeling. Earth Interactions, 2. [Available on-line at http://EarthIneractions.org]

Milly, P.C.D., 1994: Climate, soil water storage, and the average annual water balance. *Water Resources Research*, **30**(7), 2143-2156.

Mohseni, O., and H.G. Stefan, 1998: A Monthly Streamflow Model. Water Resources Research, 34(5), 1287-1298.

National Research Council (NRC), 1991: *Opportunities in the Hydrologic Sciences.* National Academy Press, Washington, D.C., 348 pp.

Natural Resources Conservation Service (NRCS), 1994: State Soil Geographic (STATSGO) Data Base: Data Use Information. U.S. Department of Agriculture, Miscellaneous Publication 1492, U.S. Department of Agriculture, Fort Worth, Texas. [Available on-line at http://www.essc.psu.edu/soil_info/]

Owe, M., Chang, A., and R.E. Golus, 1988: Estimating surface soil moisture from satellite microwave measurements and a satellite derived vegetation index. *Remote Sensing of the Environment*, **24**, 331-345.

Owe, M., de Jeu, R., and A.A. Van de Griend, 2000: Estimating long term surface soil moisture in the GCIP area from satellite microwave observations. *Proceedings Remote Sensing and Hydrology Symposium 2000,* Santa Fe, New Mexico, April 2000.

Protopapas, A., and A. P. Georgakakos, 1990: Irrigation scheduling using optimal control methods. *Water Resources Research*, 26(4), 647-670.

Roads, J.O., Chen, S.-C., Guetter, A.K., and K.P. Georgakakos, 1994: Large-scale aspects of the United States hydrologic cycle. *Bulletin of the American Meteorological Society*, **75**(9), 1589-1610.

Rodriguez-Iturbe, I., Entekhabi, D., and R.L. Bras, 1991: Nonlinear dynamics of soil moisture at climate scales, 2, Chaotic analysis. *Water Resources, Research*, **27**(8), 1907-1915.

Rodriguez-Iturbe, I., Vogel, G.K., Rigon, R., Entekhabi, D., and A. Rinaldo, 1995: On the spatial organization of soil moisture. *Geophysical Research Letters,* **22***(*20), 2757-2760.

Saxton, K.E., Johnson, H.P., and R.H. Shaw, 1974: Modeling evapotranspiration and soil moisture. Transactions of the ASAE, 17(4), 673-677.

Schaake, J.C., Koren, V.I., Duan, Q.-Y., Mitchell, K., and F. Chen, 1996: Simple water balance model for estimating runoff at different spatial and temporal scales. *J. Geophysical Research - Atmospheres,* **101**(D3), 7461-7475.

Shao, Y., and A. Hendrson-Sellers, 1996: Modeling soil moisture, A project for intercomparison of land surface parameterization schemes, Phase 2(b). *J. Geophysical Research - Atmospheres,* **101**(D3), 7225-7250.

Takle, E.S., and L.O. Mearns, 1995: Midwest temperature means, extremes and variability: Analysis of results from climate models. In *Preparing for Global Change, A Midwestern Perspective,* G.R. Carmichael, G.E. Folk, and J.L. Schnoor (eds.). SPB Academic Publishing bv, Amsterdam, The Netherlands, 133-140.

Ulaby, F.T., Dubois, P.C., and J. van Zyl, 1996: Radar mapping of surface soil moisture. *J. Hydrology,* **184**, 57-84.

van Dam, J.C., 1999: *Impacts of Climate Change and Climate Variability in Hydrological Regimes.* Cambridge University Press, New York, 137 pp.

Vinnikov, K.Y., Robock, A., Speranskaya, N.A., and C.A. Schlosser, 1996: Scales of tempoeral and spatial variability of midlatitude soil moisture. *J. Geophysical Research - Atmospheres,* **101**(D3), 7163-7174.

Vinnikov, K.Ya., and I.B. Yeserkepova, 1991: Soil moisture, Empirical data and model results. *J. Climate*, **4**, 66-79.

Walsh, J.E., Jasperson, W.H., and B. Ross, 1985: Influences of snow cover and soil moisture on monthly air temperature. *Monthly Weather Review*, **113**, 756-768.

Yates, D.N., 1997: Approaches to continental scale runoff for integrated assessment models. *J. Hydrology,* **201**, 289-310.

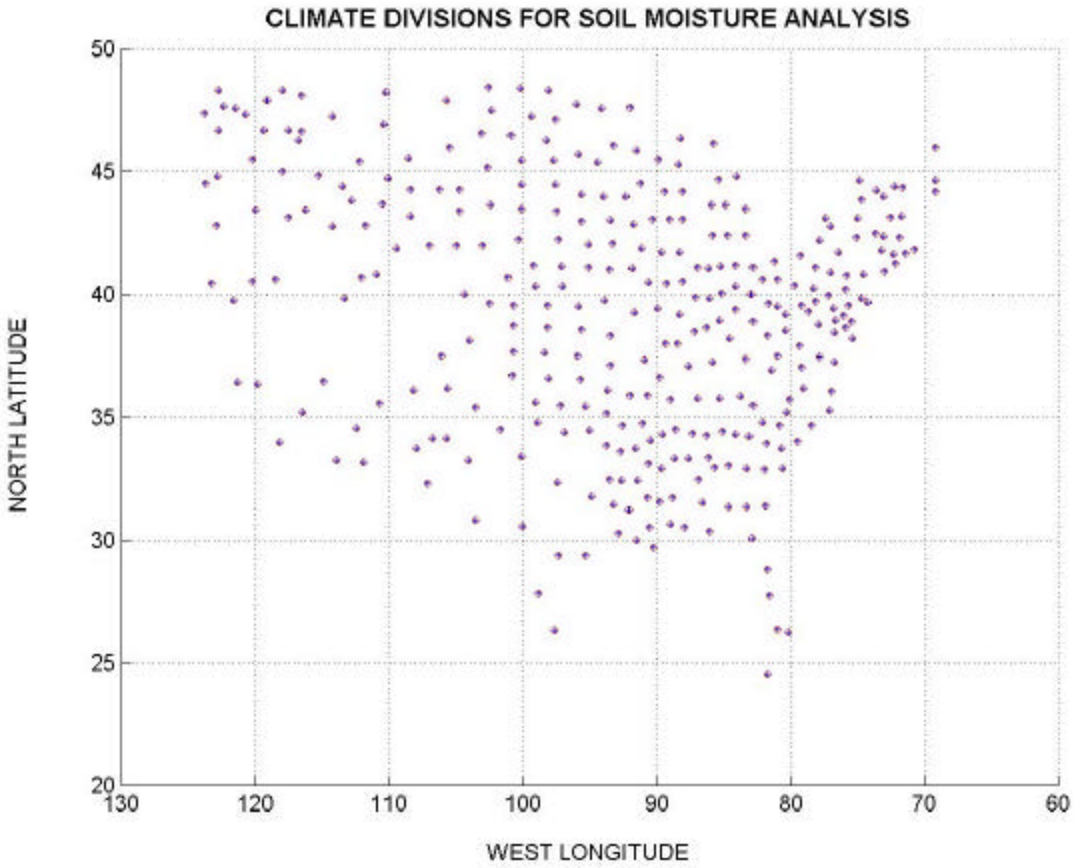

Figure 1. Longitude and latitude coordinates for the US climate divisions.

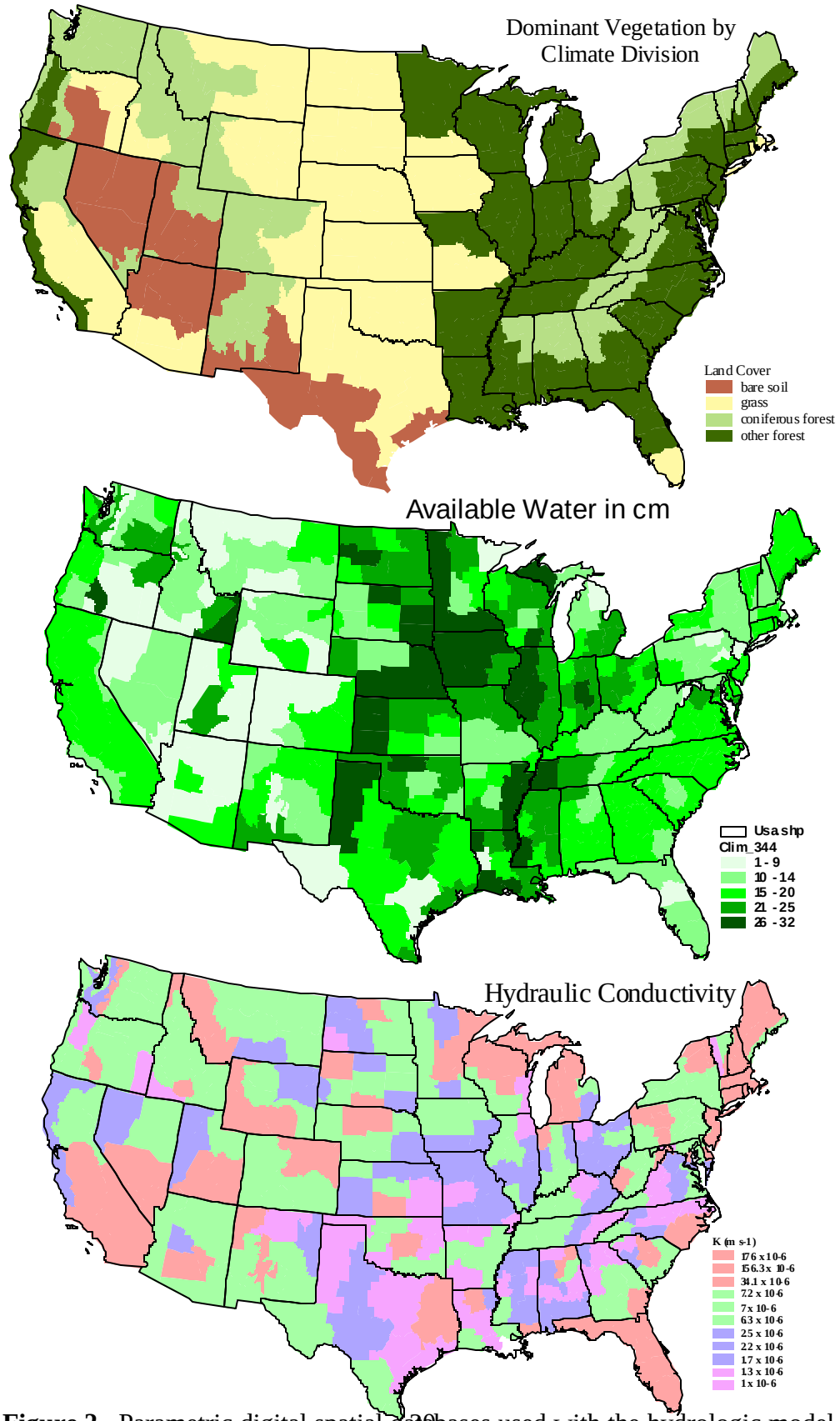

Figure 2. Parametric digital spatial databases used with the hydrologic model.

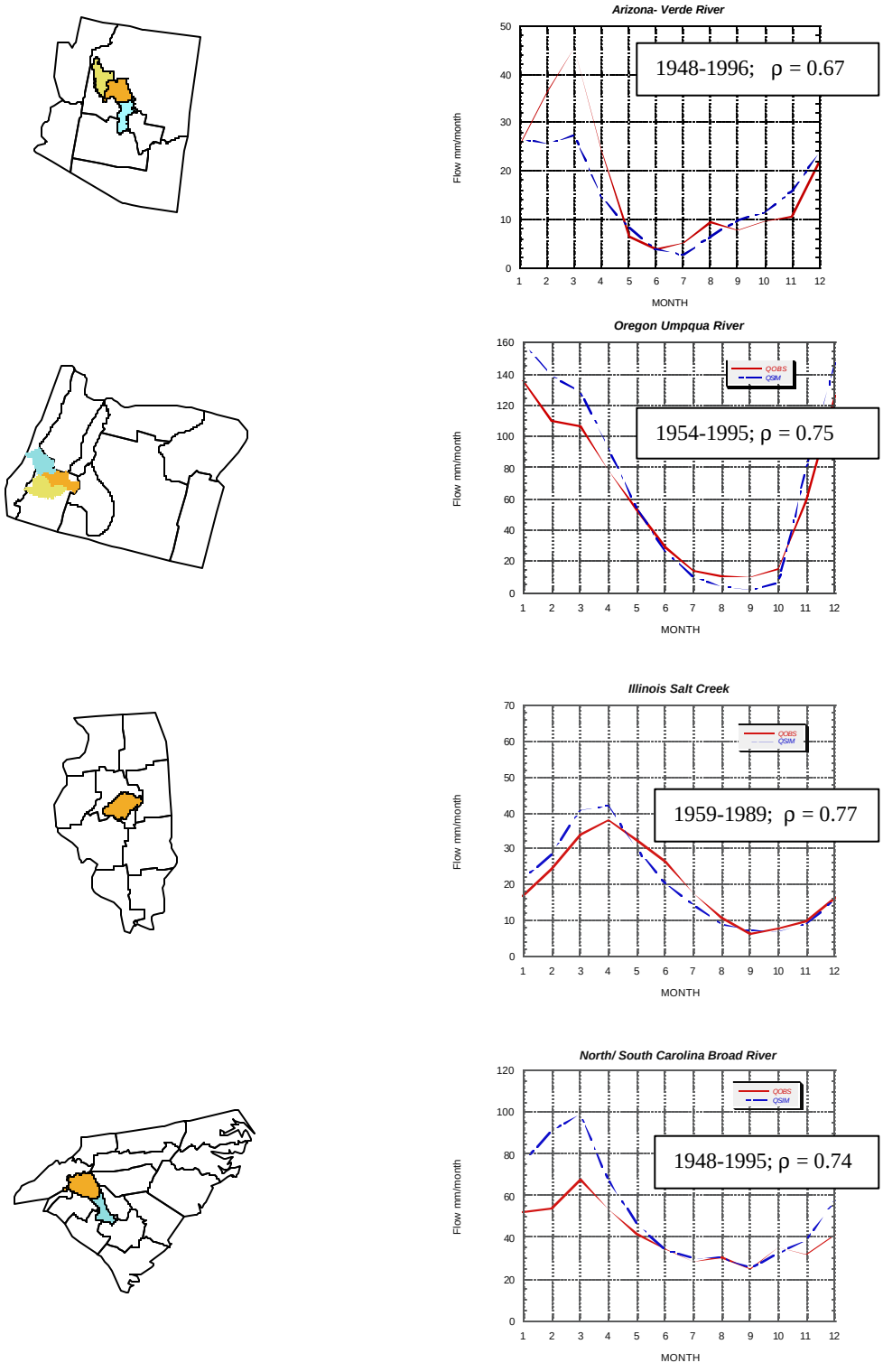

Figure 3. Long term monthly averages of observed (solid lines) and simulated (dashed-dotted lines) streamflow for Verde River, AZ, Umpqua River, OR, Salt River, IL, and Broad River, SC. Left column shows the basins in a background of nearby climate divisions. Period of record and the cross-correlation coefficients, ρ, of monthly observed and simulated anomalies are shown.

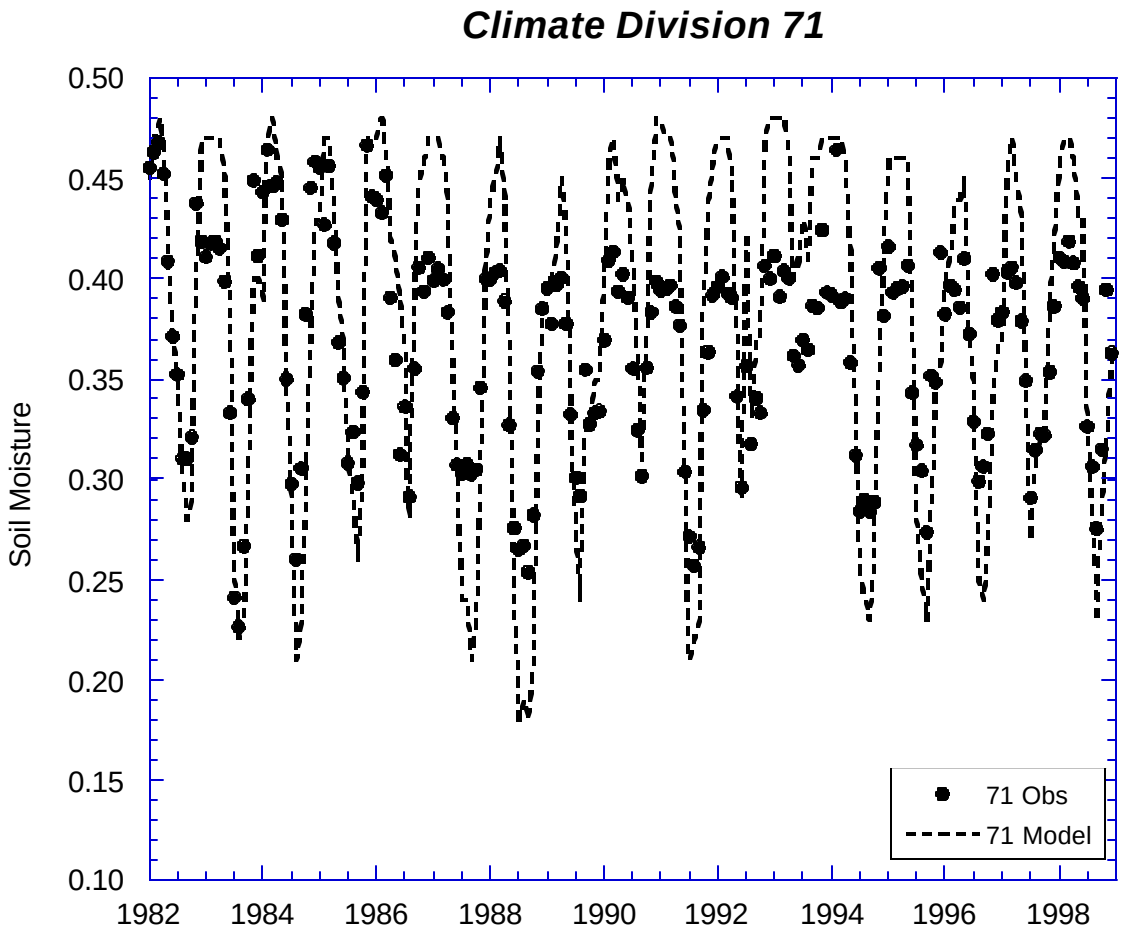

Figure 4. Observed (solid line) and simulated (dashed line) monthly soil moisture for climate division 71 in Illinois.

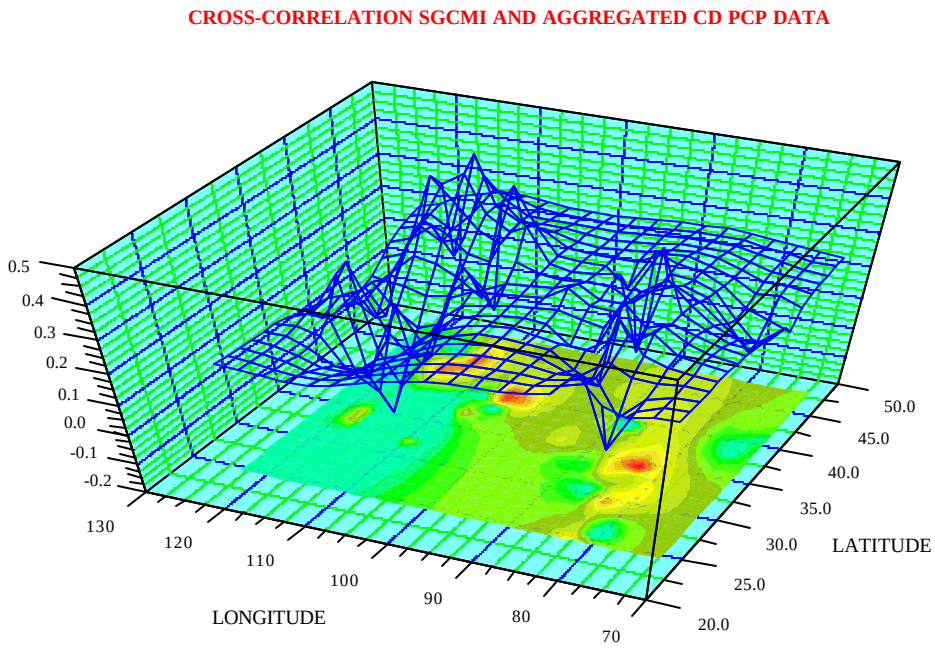

Figure 5. Cross-correlation between the climate division monthly precipitation field and the corresponding ones of the coupled climate model (CGCM1) for the historical period 1931-1996. The climate division data was spatially averaged to correspond to the climate model grid scale.

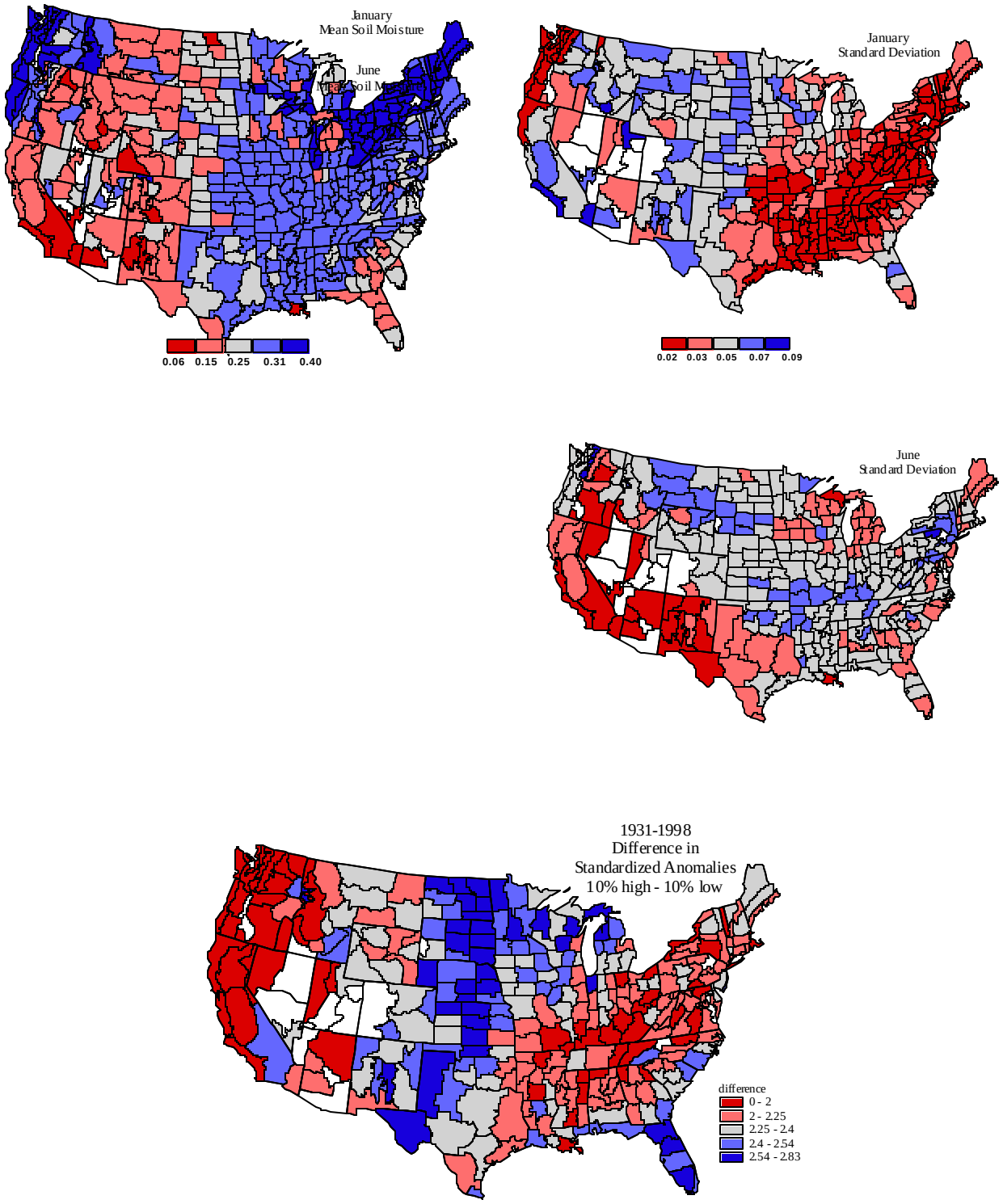

Figure 6. Means and standard deviations of soil moisture for the historical period and for January and June. Also shown are differences in high/low deciles of standardized soil moisture anomalies. Climate divisions with invalid data are shown in white.

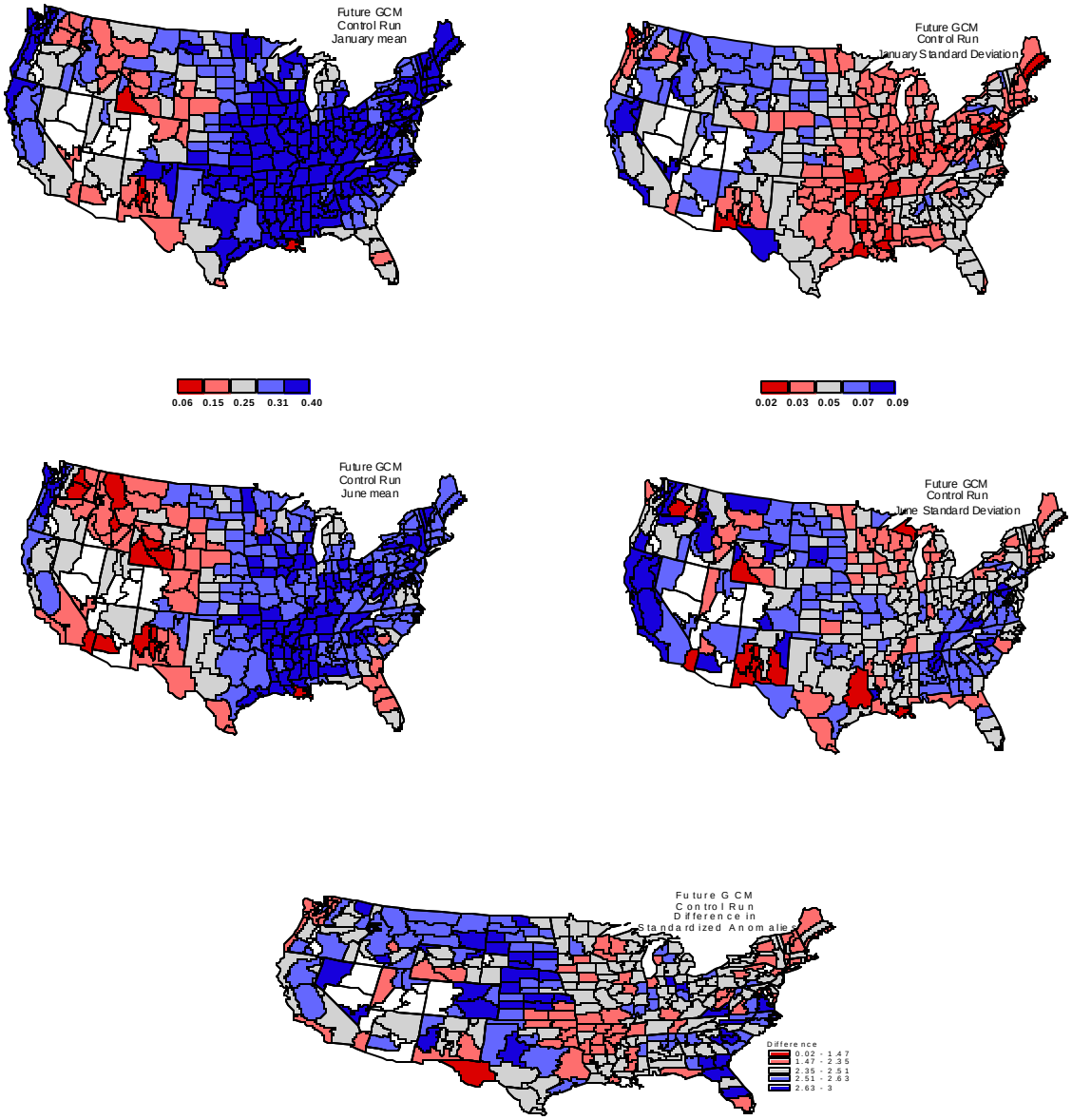

Figure 7. As in Figure 6 but for the control CGCM1 run.

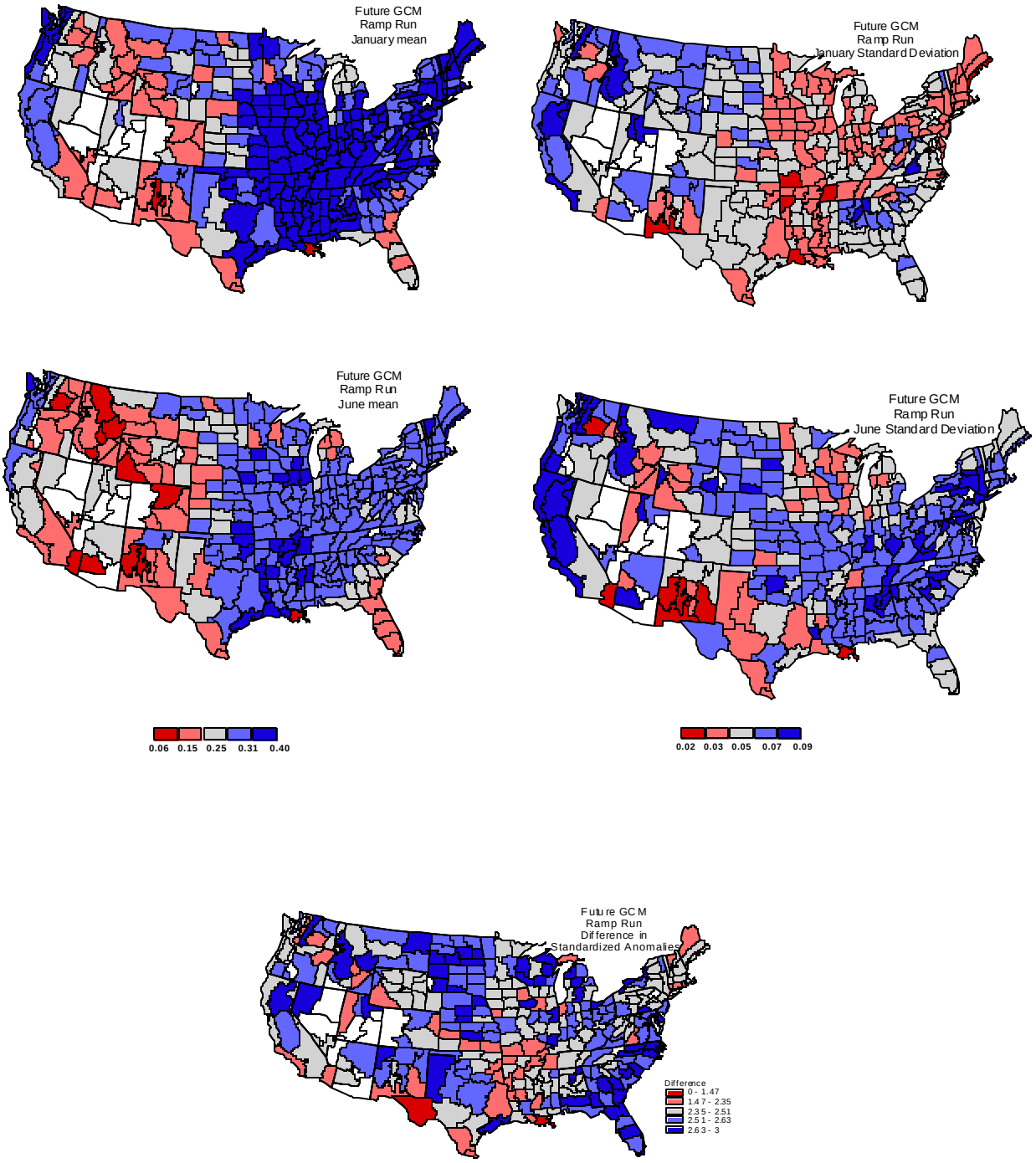

Figure 8. As in Figure 6 but for the greenhouse gas increase CGCM1 run.

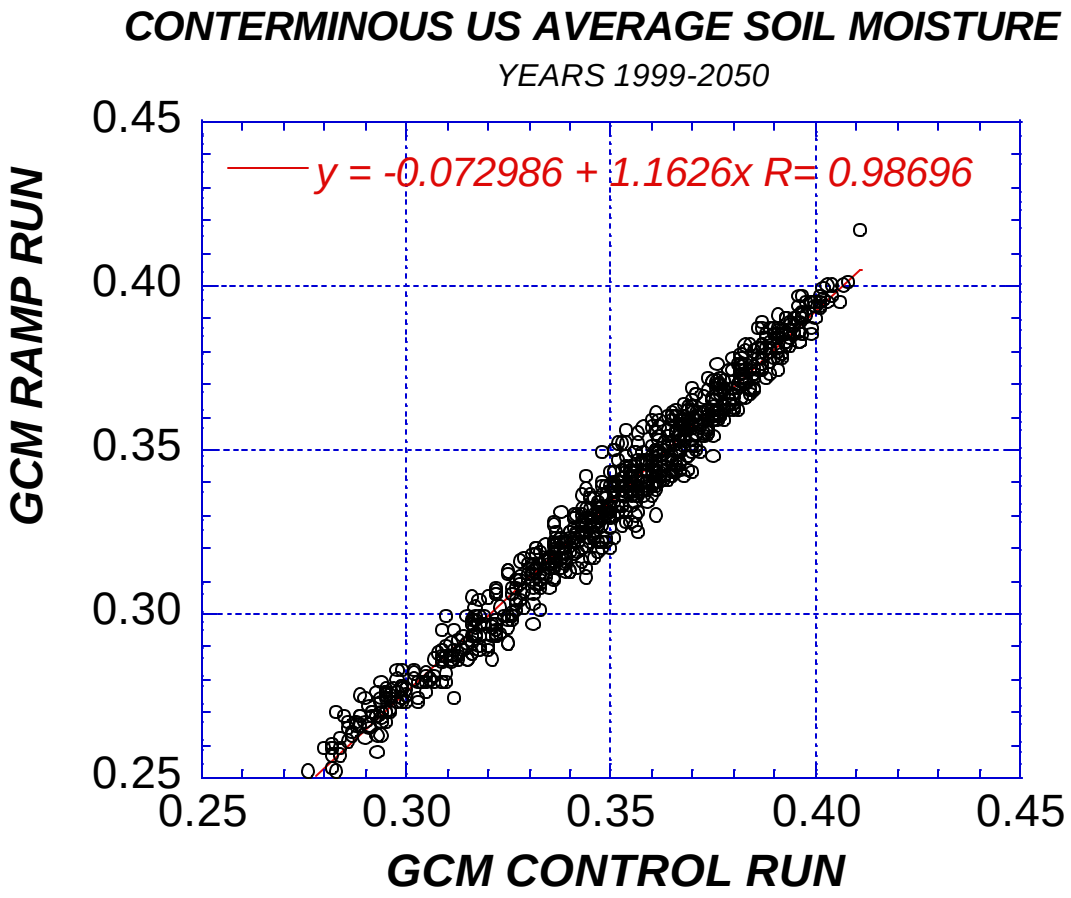

Figure 9. Association of soil moisture resulting from the CGCM1 control scenario with that resulting from the CGCM1 greenhouse gas increase scenario. Soil moisture is averaged over the coterminous US.

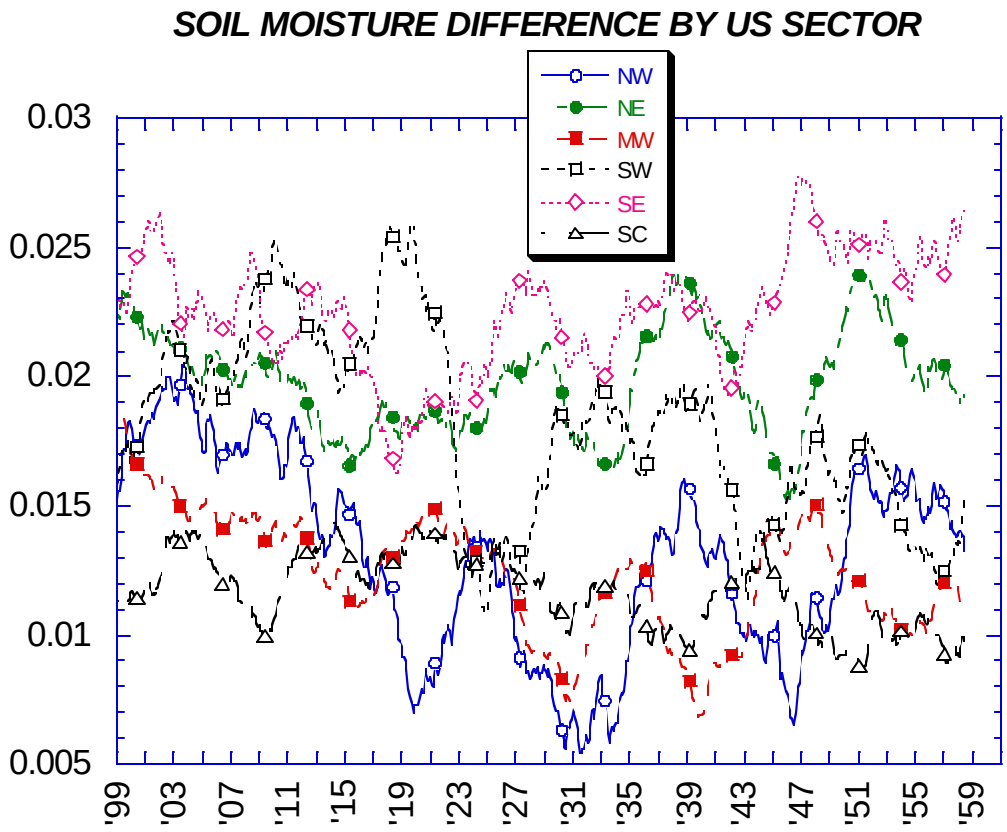

Figure 10. Smoothed differences in soil moisture resulting from the control and the greenhouse gas increase scenario by sector in the US. A 5-year smoother was applied to eliminate high frequency noise in the differences.

Table 1. Monthly Canopy Distribution and Phenology Coefficients

	f_{s_i}			f_{p_i}		
	Grass	*Conifers*	*Deciduous*	*Grass*	*Conifers*	*Deciduous*
JAN	0.5	0.5	0.5	0	0.5	0
FEB	0.5	0.4	0.5	0	0.6	0
MAR	0.5	0.3	0.5	0	0.8	0.5
APR	0.4	0.2	0.4	0	1.0	1.0
MAY	0.1	0.2	0.3	1.0	1.0	1.0
JUN	0.05	0.15	0.1	1.0	1.0	1.0
JUL	0.05	0.15	0.05	0.8	1.0	1.0
AUG	0.1	0.15	0.05	0.6	1.0	1.0
SEP	0.15	0.2	0.2	0.7	0.8	0.8
OCT	0.35	0.3	0.4	0.8	0.7	0.5
NOV	0.5	0.4	0.5	0	0.6	0
DEC	0.65	0.5	0.5	0	0.5	0

Table 2. Nominal Soil Moisture Parameter Values

Soil Class	$q_s(m^3/m^3)$	$q_f(m^3/m^3)$	$q_m(m^3/m^3)$	$K_s(m/h)$	$s_{Ks}(m/h)$	b
Sand	0.34	0.09	0.015	0.058	2.79	0.038
Loamy Sand	0.42	0.16	0.05	0.034	4.26	0.042
Sandy Loam	0.43	0.21	0.07	0.022	4.74	0.050
Loam	0.44	0.25	0.095	0.018	5.25	0.048
Silty Loam	0.48	0.29	0.11	0.017	5.33	0.044
Sandy Clay Loam	0.40	0.24	0.11	0.021	6.77	0.044
Clay Loam	0.47	0.32	0.17	0.016	8.17	0.046
Silty Clay Loam	0.46	0.33	0.19	0.015	8.72	0.046
Sandy Clay	0.41	0.29	0.18	0.026	10.73	0.035
Silty Clay	0.47	0.35	0.21	0.012	10.39	0.051
Clay	0.47	0.36	0.24	0.011	11.55	0.0472

Note: Values are based on means of Cosby et al. 1984. The symbol s_{Ks} denotes standard deviation of saturated hydraulic conductivity.

Table 3. Characteristics of Validation Sites

Basin	Climate Division*	Area km^2	Jan	Feb	Mar	Apr	May	June	July	Aug	Sept	Oct	Nov	Dec	*r*
Arizona- Verde River	11	14,000	0.2	0.3	0.3	0.5	0.4	0.4	0.2	0.2	0.2	0.2	0.2	0.2	0.67
Illinois- Salt Creek	71	4,700	1.5	1.5	1.5	1.3	1.0	0.8	0.7	0.8	0.9	1.0	1.1	1.2	0.77
Oklahoma $3^o x 3^o$ Region+	239	90,000	1.5	1.5	1.5	1.3	1.0	0.8	0.8	0.8	1.0	1.3	1.4	1.5	0.82
Oregon- Umpqua River	246	9,600	1.5	1.5	0.7	0.6	0.7	0.6	0.5	0.5	0.5	0.7	1.0	1.3	0.75
South/North Carolina- Broad River	266	7,300	1.5	1.5	1.3	1.1	0.8	0.8	0.5	0.8	0.8	1.1	1.5	1.5	0.74

* Climate division used to supply parameters to the macroscale model.

+ Region and data as referenced in *Guetter and Georgakakos (1996)*.

Table 4. Observed and Simulated Soil Moisture Statistics for Illinois

Division:	***68***	***69***	***70***	***71***	***72***	***73***	***74***	***75***	***76***	***IL***
Mean Obs	0.34	0.33	0.34	0.37	0.34	0.37	034	0.36	0.36	0.34
Mean Sim	0.40	0.41	0.38	0.38	0.39	0.38	0.38	0.38	0.39	0.38
STD Obs	0.04	0.04	0.04	0.05	0.04	0.05	0.03	0.06	0.03	0.04
STD Sim	0.07	0.07	0.08	0.08	0.07	0.08	0.08	0.09	0.08	0.07
Cross Cor	0.7	0.5	0.6	0.8	0.8	0.8	0.5	0.6	0.5	0.8